Topology Optimization and Cooling Structures for Electronic Equipment in Small Satellites

Javier Garrido, David Orgaz, Borja Cobo, and Javier Vega
Madrid Space Europe S.L., Madrid, Spain

Abstract—Data processing capacity and power demand are rapidly increasing in telecom and scientific payloads. Together with system miniaturization, this trend often leads to performance limitations caused by insufficient cooling, which can limit the revenue obtainable from flight equipment. Optimized satellite structures and cooling systems are therefore key enablers for next-generation high-throughput small satellites and future space missions. This paper presents the application of topology optimization to the design of an electronics frame for a high-power satellite application. The objective is to obtain a minimum-mass design that withstands demanding mechanical and thermal loads. The concept incorporates embedded heat pipes to improve thermal management through phase-change heat transport, and it is intended for additive manufacturing, which allows agile production of optimized geometries tailored to specific use cases. The Solid Isotropic Material with Penalization (SIMP) method was applied using HyperMesh and OptiStruct. The resulting electronics frame supports a printed circuit board inside a satellite, withstands launch mechanical loads, and dissipates heat generated by the electronic components. Compared with a conventional frame, the optimized design achieves about 15% mass reduction while the heat-pipe concept reduces critical electronic temperatures by tens of degrees Celsius, increasing the available thermal margin for higher power throughput.

Keywords—topology optimization, small satellites, electronics cooling, embedded heat pipes, additive manufacturing, SIMP, OptiStruct, thermal management.

I. INTRODUCTION

Small satellites are increasingly expected to host high-throughput telecommunication payloads, high-rate on-board data processing, and compact scientific instruments. These capabilities increase electrical power dissipation while the allowable volume and mass of the spacecraft bus remain constrained. As power density increases, the mechanical frame that supports electronics is no longer only a structural bracket; it also becomes a thermal path between heat-generating components, the printed circuit board (PCB), and the spacecraft cold interface.

In launch vehicles and small-spacecraft platforms, mass is one of the main design drivers. A reduction of a few hundred grams may translate into launch-cost savings, a larger payload allocation, or additional propellant margin. However, removing material indiscriminately can reduce stiffness, lower natural frequencies, and increase thermal gradients. The design of electronics support frames must therefore consider structural and thermal requirements together, rather than as independent late-stage verifications.

Topology optimization provides a systematic way to identify efficient material paths in a design domain. The method is especially attractive when combined with metal additive manufacturing, because the organic and branching geometries obtained from optimization are often difficult or expensive to machine conventionally. For space hardware, additive manufacturing also supports low-volume production, design customization, and the integration of functions such as embedded heat pipes, local stiffeners, cable clearances, and thermal conduction paths.

This paper summarizes the design methodology and results for an optimized satellite electronics frame. The work is based on both R&D and commercial work in which a baseline electronic frame was remodeled, optimized, and validated under mechanical and thermal load cases (currently under TVac and vibration testing). The main contribution is the combined use of topology optimization and embedded heat-pipe cooling to obtain a lightweight frame that maintains structural integrity while improving the thermal environment of the PCB and electronic components.

II. BACKGROUND

Topology optimization searches for the best distribution of material inside a prescribed design volume, subject to constraints such as stress, displacement, frequency, mass, or thermal compliance. In this work, the Solid Isotropic Material with Penalization (SIMP) method was used. The design domain is discretized into finite elements, and each element receives a relative density (ρ_e) variable between zero and one. Elements with high relative density are retained as load or heat paths, while low-density elements are candidates for removal. The SIMP interpolation penalizes intermediate densities so that the final result tends toward a manufacturable solid-void design. The elastic modulus of each element (Eq (1)) is scaled as a function of relative density, typically using a penalization (p) factor of about three. A minimum relative density is set as threshold to remove elements and the resulting part stiffness is calculated according to equation (2).

$$E(\rho_e) = \rho_e^p E_0 \qquad (1)$$

$$K_{SIMP}(\rho) = \sum_{e=1}^{N} [\rho_{\min} - (1 - \rho_{\min})\rho_e^p] K_e \qquad (2)$$

This approach makes it possible to minimize mass while maintaining stiffness and stress performance. In OptiStruct, the same framework can also support thermal optimization by using thermal compliance as a response, guiding material toward regions that reduce temperature under imposed heat loads.

On the purely thermal front, heat pipes are passive two-phase heat-transfer devices. Heat absorbed at the evaporator section vaporizes the working fluid; the vapor then travels to a colder condenser region, releases latent heat, and returns through a capillary wick. This process provides high effective thermal conductivity with no moving parts and no electrical power consumption. In a satellite electronics frame, embedded heat pipes can transport heat from local components toward a cold structural interface, reducing hot spots and lowering PCB temperature. There are already solutions with flight heritage but with the draw backs of being bulky, load-inducing on electronic component and non-optimum for AIT processes.

Additive manufacturing makes the integration of topology-optimized load paths and embedded thermal features feasible. Powder bed fusion processes can manufacture complex internal channels, local ribs, and lightweight lattices that would be challenging for conventional machining. The selected material for the frame was Scalmalloy [5], an aluminum alloy suitable for additive manufacturing and attractive for aerospace structures because of its strength-to-weight ratio.

III. REQUIREMENTS AND INITIAL MODEL

ADD PROCESS FLOW

The design target was an electronics frame that supports a critical processing PCB and interfaces with the satellite structure and with adjacent electronic frames. The initial geometry preserved the external envelope, the PCB attachment points, and the structural interfaces defined by the existing product. A solid interior design domain with a thickness of 14.5 mm was introduced so that topology optimization could identify the internal material paths needed for structural and thermal functions.

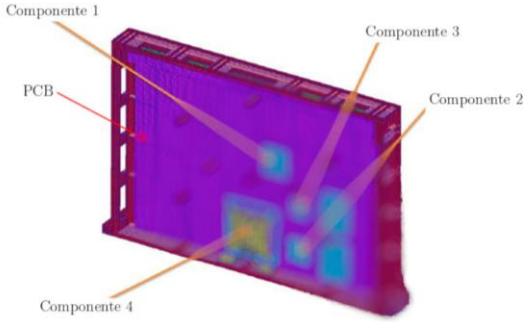

Fig. 1. PCB lay-out and initial frame design (blurred due to IP)

The structural requirements included modal (>140Hz), quasi-static load (45g applied independently along the three orthogonal axes) sinusoidal vibration, random vibration, and shock loads as in Fig 2. and 3. coming from launchers enveloping spectrum.

Freq [Hz]	Level [g]
5	1.0
30	20.0
110	20.0

Freq [Hz]	Level [g]
5	1.0
20	20.0
110	20.0

Freq (Hz)	Level
20	0.015 g^2/Hz
20 - 100	+3 dB/oct
100 - 400	0.076 g^2/Hz
400 - 2000	-3 dB/oct
2000	0.015 g^2/Hz
Over all	8.7 g rms

Freq [Hz]	Level
20	0.022 g^2/Hz
20 - 100	+3 dB/oct
100 - 400	0.11 g^2/Hz
400 - 2000	-3 dB/oct
2000	0.022 g^2/Hz
Over all	10.5 g rms

Fig. 2. Sine and Random vibration levels, in-plane (left) and out-of-plane (right)

Freq [Hz]	Level [g]
100	35
2500	750
10000	1400

Fig. 3. Shock vibration levels, applied independently on each of the three axes

Mechanical integrity was evaluated using Von Mises stress and margins of safety based on the material allowables (and after adding standard factors of safety for yield and ultimate strength of FoSy 1.1 and FoSu 1.25, KM 1.2 and KP 1.1)

The thermal requirements were defined by the heat dissipated by the PCB and four main electronic components, whose operating temperature range was specified from -40 °C to 120 °C. The thermal solution was required to transport heat toward the lower frame interface, at 50°C, and to operate without relying on gravity orientation in the flight environment. The thermal loads are summarized in the following table.

Componente	Potencia disipada [W]	Área [m^2]	Flujo calor [W/m^2]
Componente 1	2.50	$1.47 \cdot 10^{-3}$	1700
Componente 2	1.43	$5.49 \cdot 10^{-4}$	2606
Componente 3	1.57	$3.31 \cdot 10^{-4}$	4741
Componente 4	10.70	$3.32 \cdot 10^{-3}$	3221
PCB	17.87	$8.85 \cdot 10^{-2}$	202

Fig. 4. Power input per component

The mechanical finite element model was created in HyperMesh. The frame interior and external envelope were meshed mainly with three-dimensional hexahedral elements, while the satellite attachment legs were modeled with shell elements. The PCB was included as a two-dimensional finite element model rather than a point mass, because that representation better captured local displacements, stresses, and the dynamic coupling between the PCB and frame. RBE and CBUSH elements represented the bolted interfaces. The model included thermal properties to capture conductive heat flows from the components and PCB to the cold boundary at the satellite interface.

IV. OPTIMIZATION METHODOLOGY

The mechanical optimization objective was to minimize the mass of the structure while satisfying constraints on stress and frequency. The optimization recorded responses including weighted static compliance, total mass, first natural frequency, and Von Mises stress in the non-design regions. Additive manufacturing constraints were included to promote realizable geometry. In particular, material removal was constrained along the axis normal to the frame plane, matching the intended build and post-processing strategy.

The most restrictive mechanical case for the first optimization was the quasi-static load in the Z-axis. OptiStruct produced an element-density field after 85 iterations. Interpreting the density field with a relative-density threshold of 0.7 revealed clear structural branches linking the PCB attachments, frame perimeter, and satellite feet. These paths were consistent with the high-stress regions of the load case and became the basis for the mechanical ribs of the final CAD model.

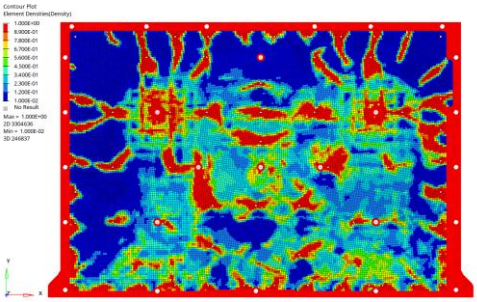

Fig. 5. Relative density map from QSL optimization in Z-axis

The thermal optimization used the thermal finite element model built from the same geometric basis. The objective was to minimize thermal gradient and limit maximum temperatures, which drives material toward regions that improve conduction between the heat sources and the cold boundary. The resulting density field showed that conduction paths were required close to the PCB heat

sources and that direct paths to the lower frame interface were more efficient than relying only on conduction around the external frame perimeter.

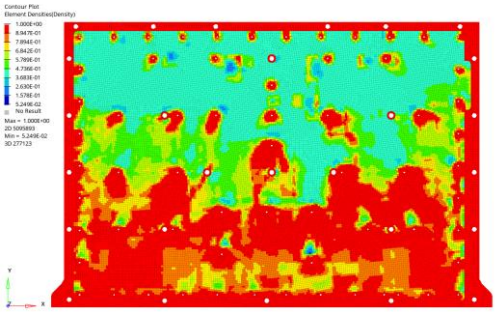

Fig. 6. Relative density map from thermal optimization

Mechanical and thermal optimization were not simply superimposed. The design process required interpretation in CAD, because some mechanical branches were best placed as taller ribs for stiffness, whereas thermal branches were thinner and positioned closer to the PCB interface for heat spreading. The final CAD model combined 8 mm-high structural branches (1 - 4mm thick) with thinner thermal conduction paths (1 - 1.5mm thick), which were added to conduct heat from the electronics toward the cold side of the frame. This version demonstrated the mass benefit of topology optimization, achieving a frame mass of 736.65 g compared with 871.22 g for the original design, a reduction of approximately 15%. Thermal non-compliances were still found at two components so the design was then improved by embedding heat pipes to further reduce hot-spot temperatures.

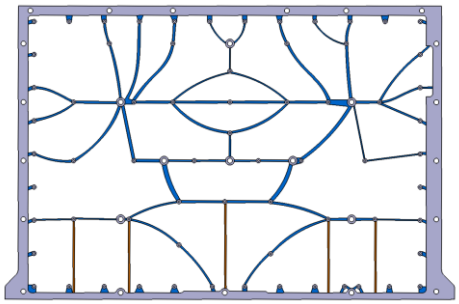

Fig. 7. 2D view of optimized CAD without heat pipes

V. FINAL DESIGN WITH EMBEDDED HEAT PIPES

The second variant introduced embedded heat pipes to improve thermal performance. Two heat pipes collected heat from the electronic-component regions and operated as evaporator/adiabatic transport sections. A third heat pipe was placed in the lower base of the frame and acted as the condenser section connected to the spacecraft cold boundary. The heat pipes replaced part of the topology-derived thermal branches and were connected to the PCB through local contact areas near the heat sources. They consist on an external casing, an internal wick/bore structure (of the same material, in this case Scalmalloy) adjacent to the casing and an internal vapour cavity. The cross section design to reach the desired heat transfer capacity while withstanding internal pressure, the geometry of interface areas of evaporator and condenser as well as the manufacturing and empirical characterization of heat pipe behaviour has been the focus of [14] and one of main R&D lines of work of Madrid Space since 2018. Thanks to several internally developed and empirically fed tools, it is possible to derive the set of geometry and working fluid parameters (type/number/size of bore/wick, foot print, filling ratio, etc.) for a given power, power density, material compatibility constraints and target heat pipe routing.

Introducing heat pipes increased thermal capability but also added mass. To compensate, material was removed while keeping structural integrity and required interfaces. The final design remained lighter than the initial frame and provided a much more direct heat-transfer path from components to the satellite structure. The final CAD mass was approximately 867gr including frame, pipes, and thermal interfaces.

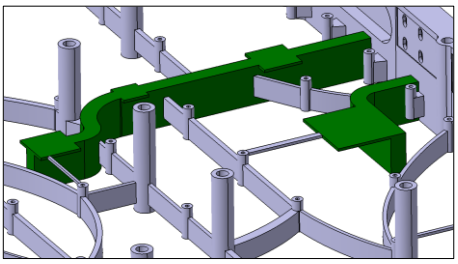

Fig. 8. Detail of heat pipes from two components: interface, routing and insertion into frame base where the third HP is found.

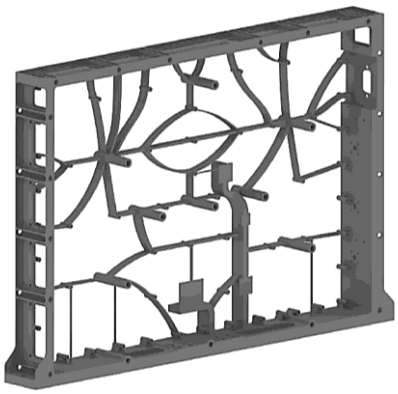

Fig. 9. Topology-derived electronics frame with embedded heat-pipe routing.

VI. VALIDATION RESULTS

The final design was validated through a sequence of mechanical checks and load FEM analyses. A free-modes check verified that the six rigid-body modes were below the 0.01 Hz criterion, confirming appropriate constraint behavior. The gravity check produced reaction forces consistent with the complete model mass. Strain-energy checks also indicated that the connections did not introduce undesired artificial stiffness.

An initial sinusoidal analysis revealed a critical issue in the out-of-plane Z direction. Although most load cases produced positive margins, the sinusoidal response of the frame had a negative margin of safety because the first natural frequency of the frame-PCB assembly was close to the frequency range of the applied load. This finding motivated a local redesign of the support regions to increase stiffness without sacrificing the main optimized architecture.

After the design modification, the first mode increased from 116.6 Hz to 140 Hz, and the maximum Z-axis sinusoidal stress in the frame decreased from 443.6 MPa to 131.8 MPa. The corresponding margin of safety changed from -0.30 to +1.35. The quasi-static and shock analyses also produced positive margins, confirming that the modified design satisfied the imposed mechanical requirements.

The thermal validation showed that the heat-pipe configuration significantly reduced component temperatures. With heat pipes, the four electronic components reached 74.86 °C, 68.21 °C, 75.35 °C, and 69.44 °C, all below the 120 °C component limit (and below the more strict 85°C from ECSSs). The maximum PCB temperature was 90.01 °C, below the 100 °C requirement. Compared with the original no-heat-pipe case, the reductions were approximately 40°C and higher for components, PCB and frame. This improvement directly increases thermal margin and supports higher power-throughput capacity.

VII. NUMERICAL SUMMARY

The optimized no-heat-pipe frame reduced the mass from 871.22 g to 736.65 g. This corresponds to a reduction of approximately 134.57 g, or about 15.4% of the original frame mass. The result is important because it was obtained while maintaining the critical mechanical interfaces and while preserving the possibility of assembling the frame with the PCB and neighboring satellite equipment.

The final heat-pipe version had a CAD mass of 867 g and a corresponding finite element mass of 0.914 kg. The difference of about 0.048 kg, or roughly 5%, is acceptable at this design stage and is mainly associated with modeling idealizations and discretization of the pipe and thermal-feature volumes. Such agreement indicates that the CAD reconstruction and the analysis model are consistent enough for preliminary design decisions.

The thermal comparison highlights the value of embedded two-phase transport. Without heat pipes, the component temperatures were 129.60 °C, 116.70 °C, 125.90 °C, and 132.90 °C, and the maximum PCB temperature was 132.90 °C. With heat pipes, the same locations decreased to 74.86 °C, 68.21 °C, 75.35 °C, and 69.44 °C, while the maximum PCB temperature decreased to 90.01 °C. The component reductions ranged from 48.49 °C to 63.46 °C.

The structural comparison before and after the local support modification also provides a clear design lesson. The first natural mode increased from 116.6 Hz to 140Hz, and the maximum stress in the critical Z-axis sinusoidal case decreased from 443.6 MPa to 131.8 MPa. The margin of safety improved from -0.30 to +1.35. This change demonstrates that targeted stiffening can recover dynamic margin with limited impact on the optimized mass distribution.

For a flight program, the reported values should be treated as analysis-based evidence that must be completed by manufacturing trials and qualification testing. Nevertheless, the margins and temperature reductions are sufficiently large to justify continued development. They indicate that an integrated topology-optimized frame can provide both launch survivability and improved electronics thermal margin in the constrained envelope of a small satellite.

VIII. DISCUSSION & CONCLUSIONS

The presented process and results support the central argument of the work: **mass reduction and thermal enhancement can be merged when the structure is designed as a multifunctional component.** Material removed from low-value regions can be reallocated to structural branches, local thermal paths, and embedded heat-pipe interfaces. The final design therefore uses mass more efficiently than the baseline frame, rather than simply minimizing mass at the expense of thermal or dynamic robustness.

The initial results pointed in different directions since structural optimization was mainly driven by launch loads and eigenfrequency requirements, while the thermal optimization introduced additional material paths to improve heat dissipation from the PCB and electronic components. For this reason, the purely mathematical design process was complemented with engineering interpretation of the optimization outputs. The final CAD model was reconstructed in CATIA V5 from the topology optimization results and then modelled and analysed in OptiStruct. This iterative loop was necessary because the first optimized design passed most analyses but did not satisfy the required minimum eigen frequency nor a positive margin in the Z-axis sinusoidal case. After a local modification in the support region, the design satisfied the required structural margins under quasi-static, sinusoidal, random, shock, and modal requirements.

The integration of heat pipes significantly improved the thermal behaviour of the electronic frame and made it a feasible design for implementation on a flight unit. Three heat pipes were embedded in the optimized structure and connected the PCB/component regions to the lower base, which acts as the cold boundary. The thermal results showed that the frame with heat pipes allowed to keep PCB and critical electronic component within their allowable temperature ranges, which was not possible with the original design nor with the design without heat pipes.

This work developed and validated a topology-optimized satellite electronic frame with embedded heat pipes. The results demonstrate that topology optimization can reduce the mass of a satellite electronic frame while maintaining structural integrity and thermal performance, achieving an optimized multi-functional component and enabling higher power throughput, which directly translates directly into higher equipment value (for the same lifetime and mass).

IX. MANUFACTURING AND IMPLEMENTATION ASPECTS: UPCOMING WORK

The work selects additive manufacturing because the topology-optimized geometry contains internal voids, complex branches, and material layouts that would be difficult or costly to manufacture using conventional methods. The selected process is Powder Bed Fusion using Direct Metal Laser Sintering.

The selected material for the electronic frame is Scalmalloy. The thesis identifies it as suitable for additive manufacturing and highlights its low density, high specific strength, corrosion behavior, anodizing capability, and thermal conductivity, which is relevant for a frame that includes embedded heat pipes and must dissipate heat from electronic components.

As a follow-up from the work presented in this paper, the frame has been built together with several other configurations of frames and stand-alone heat pipes. In-house thermal testing have shown heat transfers capacity up to 20W with 7.1W/cm2 and newer promising designs are targeting up to 73W and 10W/cm2 (even larger if volume within the unit allows for implementation). Several samples

(including a newer version of this optimized frame) will undergo an ECSS [15] qualification campaign in Q3 of 2026, including sealing and pressure tests under relevant environment (pressure cycle, leak and burst pressure tests), thermal vacuum testing and vibration testing.

Building up on the technology, Madrid Space is currently investigating the use for 3D printed vapour chambers as thermal doubler or heat spreader, avoiding the potential dry-out of a heat pipe embedded into the panel at the interface and reducing mass with respect to current copper heat spreader solutions.

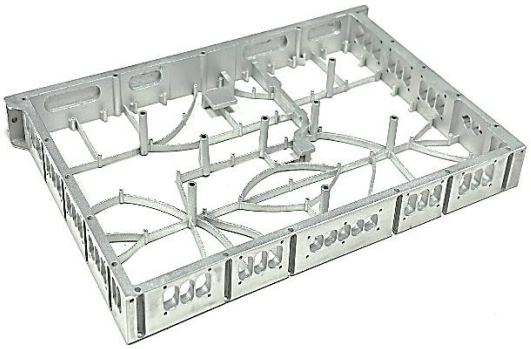

Fig. 10. First demonstrator of additive manufactured optimized frame with heat pipes embedded.

XIII. APPLICATION TO SMALL-SATELLITE PAYLOADS

The same strategy can be applied to electronic units that differ in size, heat distribution, or mounting scheme (either frames of instrument control units, power distribution units, detectors of optical instruments, etc.). The optimization domain can be adapted to each payload while keeping the customer-defined mechanical interfaces fixed. This is particularly useful in small satellites, where each mission may have a different PCB layout, power distribution, or available cold-interface location.

Because the method starts from a finite element representation, it can also include mission-specific qualification loads. A payload flying on a different launcher could update the sine, random, shock, and quasi-static inputs without changing the overall workflow. The density plots would then reveal whether the same structural branches remain valid or whether alternative paths are needed to meet the new dynamic environment.

The heat-pipe layout is similarly adaptable. For electronics with one dominant hot spot, a single evaporator route may be sufficient. For distributed processing boards, several local evaporator contacts can be connected to a shared condenser region. The final configuration should balance thermal performance with manufacturability, leak-tightness, and the risk of adding unnecessary complexity to the internal pipe network.

At spacecraft level, the optimized frame can reduce the number of separate brackets, spreaders, and thermal straps. This integration simplifies assembly and may improve reliability by reducing the number of bolted thermal interfaces. It also creates a clearer load path from the PCB to the spacecraft and a more direct heat path from the components to the radiator or cold panel.

Consequently, topology optimization should be viewed not only as a mass-reduction tool, but also as a system-integration tool. When applied early, it helps allocate material to the places where it provides the greatest combined structural and thermal benefit. This is especially relevant for high-power small-satellite payloads, where thermal positive margins, volume, and mass are all scarce resources.

REFERENCES

[1] ECSS-E-ST-32-03C, European Cooperation for Space Standardization, 2008.
[2] ECSS-E-HB-32-26A, European Cooperation for Space Standardization, 2013.
[3] EOS GmbH, Certified for Universal Success: Additive Manufacturing of Satellite Components, 2017.
[4] Altair Engineering, Practical Aspects of Optimization with Altair OptiStruct, 2021.
[5] APWORKS, Scalmalloy, 2024.
[6] C. Zhu et al., "3D printed functional nanomaterials for electrochemical energy storage," Nano Today, vol. 15, pp. 107-120, 2017.
[7] J. Ku, Introduction to Heat Pipes, 2015.
[8] Michigan Technological University, Manufacturing Engineering vs. Industrial Engineering, 2023.
[9] NASA GSFC, Ammonia-Charged Aluminum Heat Pipes with Extruded Wicks, 1999.
[10] X. Qu, N. Pagaldipti, R. Fleury, and J. Saiki, Thermal Topology Optimization in OptiStruct Software, 2016.
[11] T. G. Roberts, Cost for Space Launch to Low Earth Orbit, Aerospace Security Project, 2022.
[12] R. Simmons, FEMCI Book - Random Vibration Specification Magnitude Equations, 1997.
[13] A. Wiberg, Towards Design Automation for Additive Manufacturing: A Multidisciplinary Optimization Approach, 2019
[14] B. Cobo, Doctoral Thesis, Design and analysis of Additively Manufactured Heat Pipes
[15] ECSS-E-ST-31-02C: Two-phase heat transport equipment